Masking technique for coating thickness control on large and strongly curved aspherical optics

B. Sassolas, R. Flaminio, J. Franc, C. Michel, J.-L. Montorio, N. Morgado, L. Pinard

Masking technique for coating thickness control on large and strongly curved aspherical optics

B.Sassolas,[1,*] R. Flaminio,[1] J. Franc,[1] C.Michel,[1] J.-L.Montorio,[1] N. Morgado,[1] and L.Pinard[1]

[1]Laboratoire des Matériaux Avancés, 7 avenue Pierre de Coubertin 69100 Villeurbanne,

France

[*]Corresponding author: b.sassolas@lma.in2p3.fr

I. Abstract

This paper discusses a method to control the coating thickness deposited onto large and strongly curved optics by ion beam sputtering. The technique uses an original design of the mask used to screen part of the sputtered materials. A first multi-element mask is calculated from the measured 2D coating thickness distribution. Then, by means of an iterative process the final mask is designed. By using such a technique, it has been possible to deposit layers of tantalum pentoxide having a high thickness gradient onto a curved substrate 500 mm in diameter. Residual errors in the coating thickness profile are below 0.7%.

OCIS codes: 220.4610, 310.1860, 310.0310, 310.3840.

II. Introduction

Coating thickness control is a crucial point for interference coatings. Several applications require coating with very good thickness uniformity in order to provide constant optical properties over the optic surface. Others require pre-definite thickness profiles in order to match the coating thickness period with the light incidence angle [1]. Many masking techniques have been developed over the past ten years. Shadowing masks [2, 3] or oscillating multiaperture masks [4] were used to enhance thickness uniformity. Masks in rotation and/or

in translation were applied to manufacture linear variable interference filters [5, 6]. Most of these techniques have to deal with parameters such as the distance between the sputtering target and the substrate or the emission pattern of the sputtered material. An ingenious two rotating masks system was studied for the fabrication of annular coating with a wedge-shaped profile [7]. The latter require installing two rotating masks in front of the substrate something complex in the case of a large and curved substrate as the one considered in this paper.

In the past, two techniques were developed at Laboratoire des Matériaux Avancés (LMA) to enhance thickness uniformity on large optics: corrective coating and masking technique [8, 9]. This paper discusses an improvement of the masking technique that does not have to deal with many geometrical parameters generally involved in the models for emission patterns or any process parameter to calculate mask shape. This enhancement allows controlling the coating thickness with a precision better than 1% onto large aspherical substrates.

To perform an experimental demonstration, this technique has been applied to the deposition of a coating of tantala pentoxide onto an ellipsoidal substrate with 500 mm clear aperture and 100 mm sag. The requested coating thickness profile has a variation around 14% over the substrate aperture.

The experiment has been performed using the large Ion Beam Sputtering (IBS) coater, of 2.2x2.2x2 m^3 in size, available at LMA. The latter was designed and manufactured for the realization of the optical components for the Virgo interferometer [10].

In this paper, it is shown that the mask shape has a direct effect on the coating thickness control. The general principle is described and the procedure used to measure the

coating thickness measurement is reported. An insight of the results obtained with different masks is described and the most promising are discussed.

III.Experiment

A. Principle

The masking technique has been developed to deposit a reflective interferential coating over a spherical substrate with a 500 mm diameter clear aperture and a 900 mm radius of curvature. The final goal is to produce a large extreme ultra violet light collector. The envisaged light source is made by a dense target, placed in the focus of the mirror, and excited by a pulsed laser beam passing through a hole in the center of the mirror. This 40 mm in diameter hole will be useful in our case to hold the mask. The radiation emitted by the target is collected and focused by the mirror. The envisaged reflective coating is a multilayer stack of two materials having very close optical index. Due to the low index contrast, the reflectivity peak of the multilayer is narrow and very sensitive to incidence angle. Hence, to obtain an high reflectivity, the coating thickness profile has to match with the incident angle over the aperture of the optic (see. Figure 1). The two materials to be deposited onto the collector, have a sputtering emission pattern similar to that of tantala. For practical reasons, the demonstration of the masking technique developed to obtain the required gradient (Figure 1) has been performed with a tantala layer.

The principle adopted consists in using a correction mask fixed inside the deposition chamber in order to control the coating thickness profiles on a rotating substrate. The sputtered particles from the deposition target get through the fixed mask. Of course, with this technique, the coating profiles must have revolution symmetry. Figure 2(a) shows the experimental lay out. For a given radius r, the mask hides an angular range $[-\omega(r),\omega(r)]$ (

Figure 2(b)) and the total thickness deposited over the whole rotating substrate is decreased. The shape of the mask, i.e. the angle ω as a function of the radius r is determined by the following equation

$$e\ (r) = \frac{\int_{\omega}^{2\pi-\omega} e_{stat}(r,\theta).d\theta}{\int_{0}^{2\pi} e_{stat}(r_{max},\theta).d\theta}.e(r_{max}) \qquad (1)$$

where e(r) is the desired coating thickness profile and $e_{stat}(r,\theta)$ is the coating thickness distribution at polar coordinates (r,θ) onto an unmasked static substrate. r_{max} is the radius where e(r) is maximum. More general considerations about this point could be found in Ref. [3].

In Eq. (1), the mask is assumed infinitely close to substrate. In practice, the mask should be as close as possible to the substrate surface. For non plane substrates, the mask must be bent in two directions something more difficult and expensive to realize. It is easier to bend the mask in only one direction. As a consequence if the mask is too wide, it may hit the substrate (Figure 3(a)) contrary to what happens with a narrow mask (Figure 3(b)). Therefore a wide mask has to be moved away from the substrate surface thus reducing the masking efficiency.

To reduce the mask width, an original design has been conceived inside the laboratory. The idea involves segmenting the large mask in many thinner masks with the same symmetry (petal-like elements). The width of each petal decreases as the number of petals is increased and as a consequence they may be closer to substrate. The Equation 1 is modified to calculate the shape of an N-petals mask as follows:

$$e\ (r)=\sum_{k=1}^{N}\left(\int_{2(k-1)\pi/N+\omega}^{2k\pi/N-\omega}e_{stat}(r,\theta).d\theta\right).\frac{e\ (r_{max})}{\int_{0}^{2\pi}e_{stat}(r_{max},\theta)d\theta}\qquad(2)$$

where e(r) is desired thickness profile, $e_{stat}(r,\theta)$ is static thickness distribution at polar coordinates (r,θ) onto non rotating substrate and r_{max} is the radius where e(r) is maximum.

B. Thickness measurements

The mask described in this paper was developed by an iterative process. It means that the initial mask was calculated from the measured coating thickness distribution onto the whole substrate in static conditions. Then the successive masks were designed from the previous results. Therefore, a fake mirror was made to measure the coating thickness distribution both in static conditions and in rotation. It reproduced the curvature of the real mirror as described in Section III.A. Microscope cover glass slides (size 24 x 60 x 0.150 mm) were fixed on the fake mirror. Their thickness allowed them to bend according to the mirror curvature. Fake mirror and glass slides are shown in Figure 4.

A spectrophotometer (Perkin-Elmer, Lambda 19) was used to measure the thickness of the coating deposited on the glass slides. The refractive index of tantalum pentoxyde vs wavelength was first evaluated from the transmission spectrum using the envelop method developed by Swanepoel [11, 12]. Then, these results were used as starting values for numerical optimization between experimental and computed transmission values. Both the substrate and the coating were modeled as non absorbing materials (extinction coefficient about 1e-8). The refractive index values were fitted following the Cauchy law in the 400 to 1000 nm wavelength range

$$n_{film} = a + \frac{b}{\lambda^2} + \frac{c}{\lambda^4} \quad (3)$$

Where a,b,c are the Cauchy parameters. Tantalum pentoxyde index of refraction has been considered constant on the whole mirror and reproducible from one run to another. Afterwards we used this index law to calculate the transmission spectrum (400-1000 nm wavelength range) for tantalum pentoxide layer onto each glass slide. The differences observed in transmission spectra are caused by layer thickness variations and are used to deduce the actual thickness. The results of the fit for one of these measurements are shown on Figure 5. Theory about transmission calculation is described in [13].

Each glass slide has been measured at 6 different points along medial axis. A Matlab [14] code was developed to automate the optimization procedure described above.

IV.   Results and discussion

To show how the method works, a tantalum pentoxide layer following the profile represented in Figure 1 has been considered. The 2D coating thickness distribution on a static substrate is deduced from the measurement of the coating thicknesses on the fake linear mirror. To this purpose four different coating runs were made with the fake mirror placed along four different directions (horizontal, vertical and the 2 diagonals). The four coating thicknesses measurements are shown in Figure 6. We took the center as normalization point because it is the only point common to all the measurements. To follow the evolution of successive results and to compare with the desired profile, we kept the center as normalization point. The center is the "reference" point.

6

The thickness profile shows symmetry with respect to horizontal plane. This is confirmed by the measurements made along the diagonal directions which differ by less than 2%. Then, the 2D coating thickness distribution on the whole substrate is spline cubic interpolated from the four measurements (see Figure 7). It can be observed a thicker deposition on "the left" of mirror and noted that the variations are around 20%.

The first monolithic mask calculated from the static thickness distribution is shown in Figure 8. Due to its large width, around 120 mm, the mask has to be placed at 20 mm far from the substrate surface. At such a distance, the mask efficiency is reduced because sputtered material can pass between the mask and the substrate.

Table 1 gives the size of possible masks assuming different number of petals. The second and third columns show respectively the width of each petal and the minimal achievable gap between the petal and the substrate. The mask composed by five petals can be placed at a distance from the substrate less than 0.2 mm. However we chose the four symmetrical petals mask since it appears to be the best compromise between realization ability and efficiency. The produced mask is shown in Figure 9(a). To align the fake substrate and the mask, both are mounted on the same axis. During the coating deposition, the substrate is in rotation whereas the mask is fixed. A ball bearing system allows both parts to move independently. The assembly is represented in Figure 9(b).

The coating has been realized onto the rotating fake mirror with mask M0 (shown in grey in Figure 10). A good agreement between the experimental and the desired profiles was achieved. The difference after this first step was already below 1%. This result shows the good control of the technique even with the first mask. A second mask, called M1 and shown

in black in Figure 10, was calculated from the results obtained with M0. Notice that the petals of M1 are 1.5 mm narrower than the M0 ones.

Figure 11 shows the coating thickness on the mirror vs the curvilinear abscissa, obtained without the mask and when the mask M1 was used. The coating thickness profile that looked as a "dome" without mask was changed in a bowl-like profile. The average difference between the desired profile and the one obtained with mask M1 is 0.32 % whereas it was 0.38% with mask M0. The differences are always below 0.7% except for one of the mirror ends (abscissa -251.35 mm). This may be explained by a wrong mask positioning.

In two iterations, the multi-petals mask allows to control the coating thickness profiles with a precision better than 0.7%. The quick convergence of the iterative process is the result of several factors such as the precise measurement of the coating thickness, the positioning of the mask close to the substrate, the precise measurement of the unmasked coating thickness 2D distribution and, last but not least, the good reproducibility of the deposited coating from one run to the other.

V. Conclusion

A technique has been demonstrated for controlling thickness profile of deposited thin film. A multi-petal mask was developed to correct the coating thickness distribution onto substrate of 500 mm diameter and 100 mm sag. Overall the first results presented in this work show that the petal mask is a promising process for high coating thickness control. Using the coating thickness distribution onto the fake mirror and the desired

thickness profile, the mask shape can be computed. With four measurements of the 2D coating thickness distribution and then two masking steps the coating thickness has been controlled with a precision better than 0.7%. In conclusion, we propose a simple, quick and very efficient technique to deposit any radial gradient coating on any substrate geometry.

Acknowledgments:

References:

1. R. M. Ythier, X. Bozec, R. Geyl, A. Rinchet, C. Hecquet, M.-F. Ravet-Krill, F. Delmotte, B. Sassolas, R. Flaminio, J.-M. Mackowski, C. Michel, J.-L. Montorio, N. Morgado, L. Pinard, and E. Romeo, "EUV near normal incidence collector development at SAGEM," in *Emerging Lithographic Technologies XII*, Proc. SPIE **6921**, 692135-692111 (2008).

2. G. I. Abzalova, R. S. Sabirov, and A. V. Mikhailov, "Depositing uniform-thickness coatings on large surfaces by means of electron-beam evaporation in vacuum," J. Opt. Technol. **72**, 799-801 (2005).

3. F. Villa, A. Martínez, and L. E. Regalado, "Correction Masks for Thickness Uniformity in Large-Area Thin Films," Appl. Opt. **39**, 1602-1610 (2000).

4. J. W. Arkwright, "Fabrication of optical elements with better than [lambda]/1000 thickness uniformity by thin-film deposition through a multi-aperture mask," Thin Solid Films **515**, 854-858 (2006).

5. Pan J., Zhan F., and Yan Y., "Mask designing of linear variable filters," SPIE **2364**, 225-228 (1994).

6. L. Abel-Tibérini, F. Lemarquis, and M. Lequime, "Masking mechanisms applied to thin-film coatings for the manufacturing of linear variable filters for two-dimensional array detectors," Appl. Opt. **47**, 5706-5714 (2008).

7. Martsinovskii V.A., Safiullin F.Kh., Znamenskii M.Yu., and N. I.Kh., "Conditions for producing asymmetrical annular coatings having a wedge-shaped profile," Sov. J. Opt. Technol. **51**, 511-514 (1984).

8. B. Cimma, D. Forest, P. Ganau, B. Lagrange, J.-M. Mackowski, C. Michel, J.-L. Montorio, N. Morgado, R. Pignard, L. Pinard, and A. Remillieux, "Ion beam

sputtering coatings on large substrates: toward an improvement of the mechanical and optical performances," Appl. Opt. **45**, 1436-1439 (2006).

9. J. Agresti, E. D'Ambrosio, R. DeSalvo, J. Mackowski, A. Remillieux, B. Simoni, M. Tarallo, and P. Willems, "Flat top beam profile cavity prototype," in *Laser Beam Shaping VI*, SPIE **5876**, 58760X-58769 (2005).

10. F. Beauville, D. Buskulic, R. Flaminio, F. Marion, A. Masserot, L.Massonnet , B. Mours, F. Moreau, J. Ramonet, D. V. E. Tournefier, O. Veziant,M. Yvert, V. D. R. Barillé, D. Enard,F. Frasconi,A. Gennai,P. La Penna,M. Loupias ,, F. Paoletti, G. C. L. Bracci, E. Campagna,G. Conforto,E. Cuoco,I. Fiori,G. Guidi ,, F. M. G. Losurdo, M. Mazzoni,B. Perniola,R. Stanga,F. Vetrano,A. Viceré, G. G. D.Babusci, N. M. J.-M. Mackowski, L. Pinard, A.Remillieux, F. B. F. Acernese, E. Calloni,R. De Rosa,L. Di Fiore,A. Eleuteri,L. Milano ,, I. R. K. Qipiani, G. Russo,S. Solimeno,M. Varvella, A. B. F. Bondu, E. Chassande-Mottin,F. Cleva,T. Cokelaer,J.-P. Coulon ,, J.-D. F. B. Dujardin, H. Heitmann,C. N. Man,F. Mornet,J. Pacheco,A. Pai,H., J.-Y. V. Trinquet, M. B. N. Arnaud, M.A. Bizouard,V. Brisson,F. Cavalier,M. Davier,P. Hello,P., S. K. Heusse, V. L. C. Boccara, J. Moreau, V. Reita, L. B. P. Amico, L. Gammaitoni, M. Punturo, F. Travasso, H. Vocca, S. B. L. Barsotti, C. Bradaschia, G. Cella, C. Corda, A. Di Virgilio,, F. F. I. Ferrante, A. Giazotto, E. Majorana,L. Holloway, R. Passaquieti,, R. P. D. Passuello, A. Toncelli, M. Tonelli, and S. F. L. Brocco, C. Palomba, P. Puppo, P. Rapagnani, F. Ricci, "Low loss coatings for the VIRGO large mirrors," in *Advances in Optical Thin Films*, Proc. SPIE **5250**, 483-492 (2004).

11. R. Swanepoel, "Determination of the thickness and optical constants of amorphous silicon," J. Phys. E: Sci. Instrum. **16**, 1214-1222 (1983).

12. M.Kubinyi, N.Benkö, A.Grofcsik, and W.J.Jones, "Determination of the thickness and optical constants of thin films from transmission spectra," Thin Solid Film **286**, 164-169 (1996).

13. H.A.McLeod, ed., *Thin film optical filters* Adam Hilger Ltd, Bristol ed.
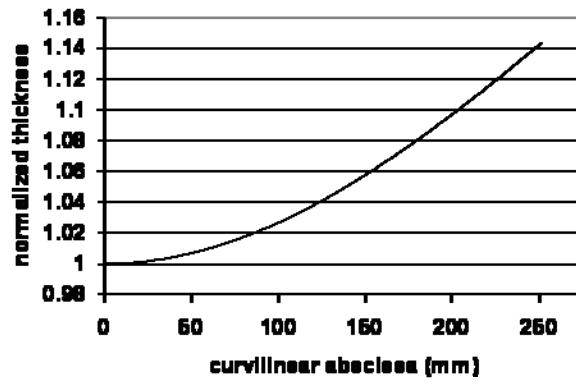
14. MATLAB, Matworks.

List of figures:

Figure 1: Theoretical thickness profile as a function of radius.

Figure 2 : (a) general masking principle: sputtered particles get through a fixed mask. (b) for radius r mask stops particles in angular range [0, ω(r)].

Figure 3 : Substrate with two masks of different width. (a) a wide mask may strike substrate contrary to (b) a thin one. Each one is placed at the same distance of the substrate surface.
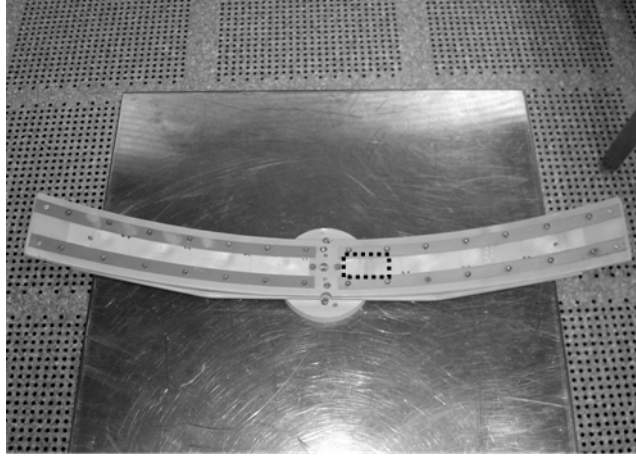
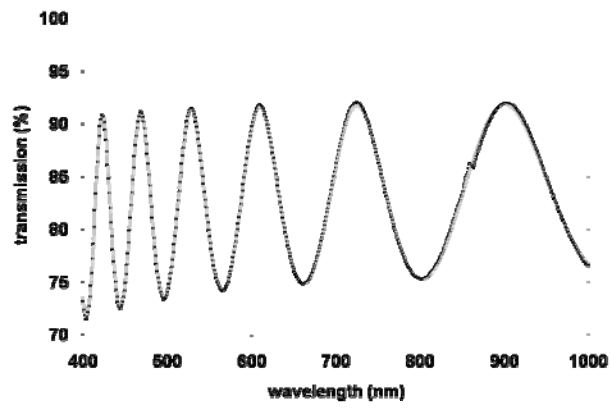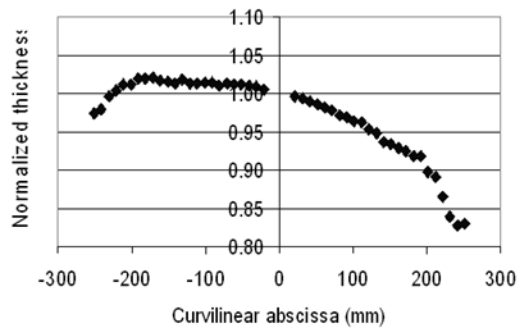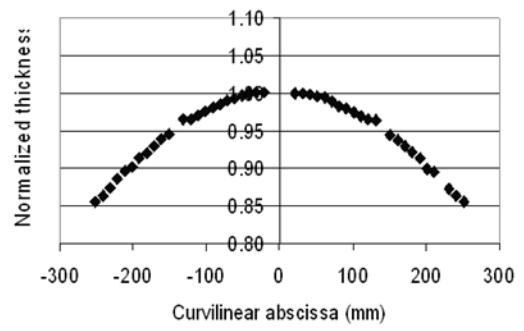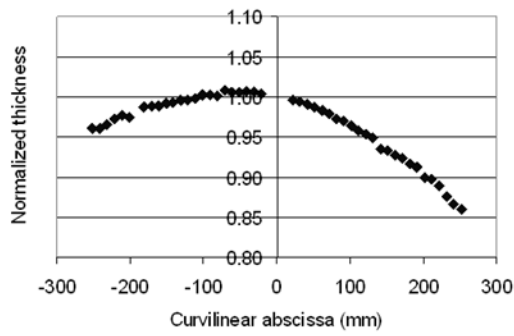Figure 4 : Fake mirror with 8 glass slides (one slide is represented by dotted rectangle)

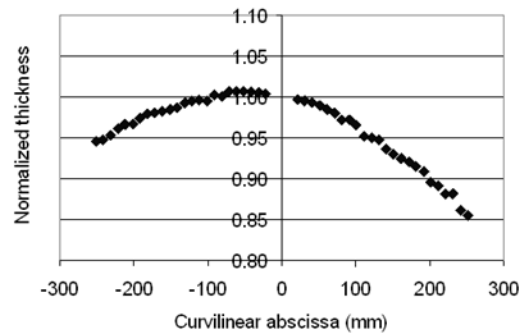Figure 5 : Experimental (dotted line) and calculated (grey line) transmission spectra.

Figure 6 : Normalized thickness profiles on (a) horizontal axis, (b) vertical axis, (c) diagonal at -45° and (d) diagonal at +45°
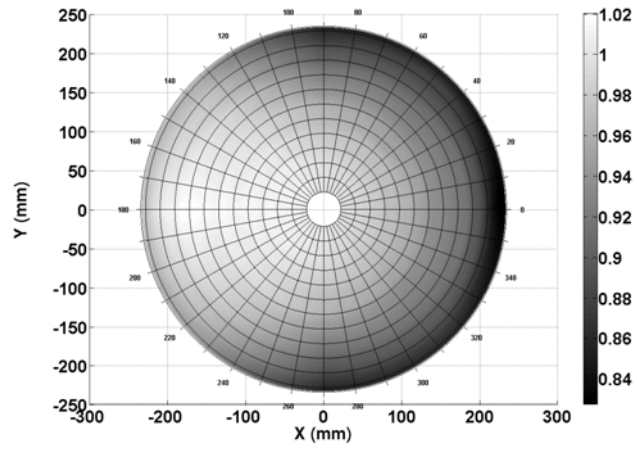
Figure 7: Normalized thickness distribution onto whole mirror after interpolation of 4 directions measurements.

Figure 8 : Monolithic mask

Figure 9 :   (a) assembly of petals and (b) installation in coater with fake mirror

Figure 10 : Petal shape for mask M0 and M1

Figure 11 : Normalized thickness profiles

Figure 1: Theoretical thickness profile as a function of radius

14

Figure 2 : (a) general masking principle: sputtered particles get through a fixed mask. (b) for radius r mask stops particles in angular range [-ω(r), ω(r)]

Figure 3 : Substrate with two masks of different width. (a) a wide mask may strike substrate contrary to (b) a thin one. Each one is placed at the same distance of the substrate surface

Figure 4 : Fake mirror with 8 glass slides (one slide is represented by dotted rectangle)

Figure 5 : Experimental (dotted line) and calculated (grey line) transmission spectra

Figure 6 : Normalized thickness profiles on (a) horizontal axis, (b) vertical axis, (c) diagonal at -45° and (d) diagonal at +45°

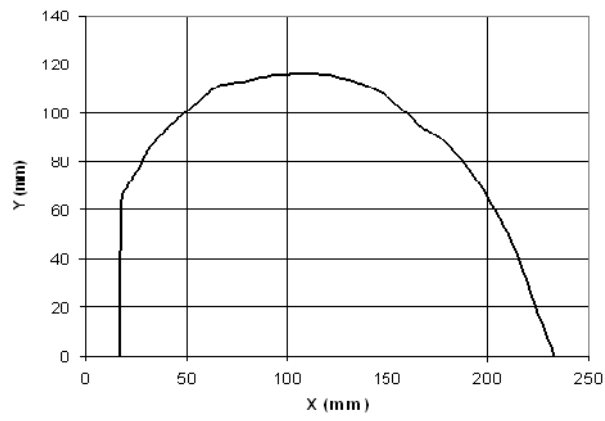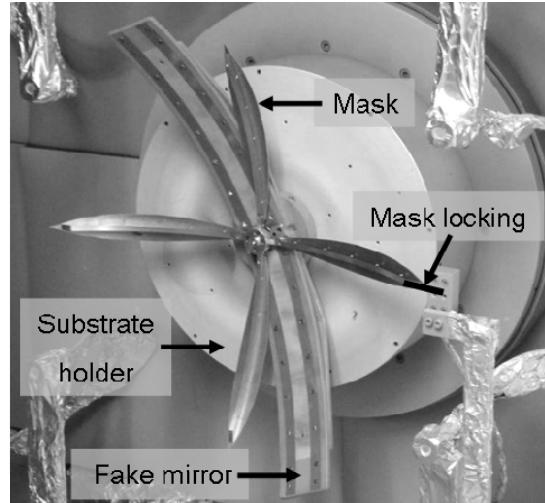**Figure 7: Normalized thickness distribution onto whole mirror after interpolation of 4 directions measurements**
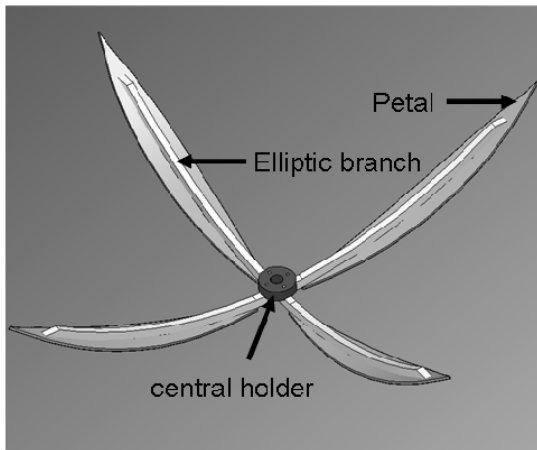
Figure 8 : Monolithic mask

Figure 9 : (a) assembly of petals and (b) installation in coater with fake mirror
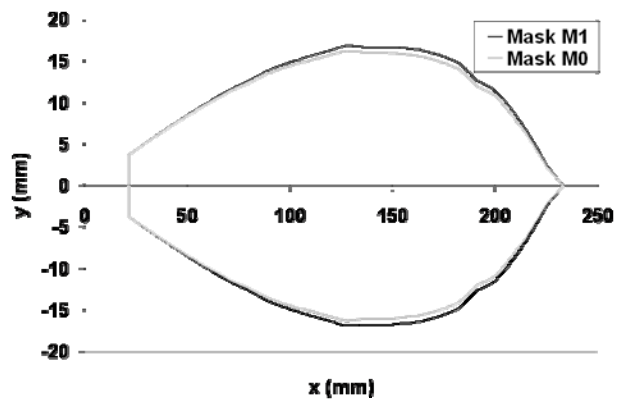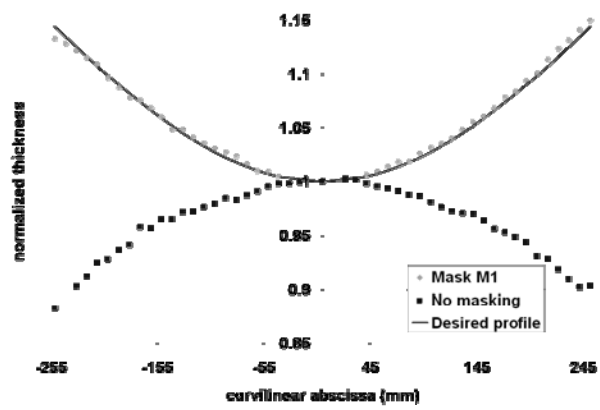
Figure 10 : Petal shape for mask M0 and M1

Figure 11 : Normalized thickness profiles

Tables:

Table 1 : Width and minimal gap between mask and substrate for different mask type

Mask type	Width (mm)	Minimal gap (mm)
Monolithic	116.51	19.53
Monolithic and symmetric	127.82	5.89
2 symmetric petals	63.88	1.38
3 symmetric petals	43.22	0.57
4 symmetric petals	32.46	0.27
5 symmetric petals	26.02	0.17